AFRL-AFOSR-VA-TR-2023-0228

Designing Structural Batteries with High Energy Density and Enhanced Safety

Yuan Yang
THE TRUSTEES OF COLUMBIA UNIVERSITY IN THE CITY OF NEW YORK
116TH AND BDWY
NEW YORK, NY,
US

12/14/2022
Final Technical Report

Air Force Research Laboratory
Air Force Office of Scientific Research
Arlington, Virginia 22203
Air Force Materiel Command

REPORT DOCUMENTATION PAGE

PLEASE DO NOT RETURN YOUR FORM TO THE ABOVE ORGANIZATION.

1. REPORT DATE	2. REPORT TYPE	3. DATES COVERED	
20221214	Final	START DATE 20200720	END DATE 20220719

4. TITLE AND SUBTITLE
Designing Structural Batteries with High Energy Density and Enhanced Safety

5a. CONTRACT NUMBER	5b. GRANT NUMBER	5c. PROGRAM ELEMENT NUMBER
	FA9550-20-1-0233	61102F
5d. PROJECT NUMBER	**5e. TASK NUMBER**	**5f. WORK UNIT NUMBER**

6. AUTHOR(S)
Yuan Yang

7. PERFORMING ORGANIZATION NAME(S) AND ADDRESS(ES)
THE TRUSTEES OF COLUMBIA UNIVERSITY IN THE CITY OF NEW YORK
116TH AND BDWY
NEW YORK, NY
US

8. PERFORMING ORGANIZATION REPORT NUMBER

9. SPONSORING/MONITORING AGENCY NAME(S) AND ADDRESS(ES)	10. SPONSOR/MONITOR'S ACRONYM(S)	11. SPONSOR/MONITOR'S REPORT NUMBER(S)
Air Force Office of Scientific Research 875 N. Randolph St. Room 3112 Arlington, VA 22203	AFRL/AFOSR RTA1	AFRL-AFOSR-VA-TR-2023-0228

12. DISTRIBUTION/AVAILABILITY STATEMENT
A Distribution Unlimited: PB Public Release

13. SUPPLEMENTARY NOTES

14. ABSTRACT
In this project, we mainly focused on tasks 1 and 3. For task 1, we developed a scalable tree-root-like lamination at the electrode/separator interface with porous fluoropolymers, which enhances load transfer from one component to another. Such interfacial adhesion dramatically enhances the flexural modulus of pouch cells by 10 times, from 0.28 GPa to 3.1 GPa. On the other side, such modification does not compromise the electrochemical performance of corresponding cells. An NMC/graphite full cell with such interfacial lamination delivers a steady discharge capacity of 151.4 mAh g-1 at C/2 and 141.9 mAh g-1 after 500 cycles. Moreover, the specific energy only decreases by 3-4%, which is the smallest reduction reported so far in structural batteries. A prototype of “electric wings” was also demonstrated, which allows an aircraft model to fly steadily.
Besides such interfacial adhesion, we also explored multiple polymer electrolytes for enhancing load transfer when electrolyte presented, including epoxy, poly(vinyl carbonate) and polyacrylate. 10-20 X enhancement of mechanical properties are observed while electrochemical cells can be cycled. After evaluation, we decide to focus on the polyacrylate electrolyte, which will be carried in the next round of this project (2022-2024), The results are described in section 4 in the progress details.

15. SUBJECT TERMS

16. SECURITY CLASSIFICATION OF:			17. LIMITATION OF ABSTRACT	18. NUMBER OF PAGES
a. REPORT	b. ABSTRACT	c. THIS PAGE		
U	U	U	UU	14

19a. NAME OF RESPONSIBLE PERSON	19b. PHONE NUMBER *(Include area code)*
MITAT BIRKAN	426-7234

Designing Structural Batteries with High Energy Density and Enhanced Safety

Grant No.: FA9550-20-1-0233

PI: Yuan Yang (Columbia University) Project Period: 08/01/2020 – 07/31/2022

Project Goals

The goal of this research is to **develop structural batteries for lightweight aerial systems and understand their mechanical and electrochemical behaviors**. There are three major goals: 1) Enhancing load transfer between different layers inside a battery. 2) Fabrication of battery electrodes with excellent mechanical properties, such as high tensile strength/modulus and high bending stiffness. 3) Simulating mechanical deformation in structural batteries.

Summary of Major Achievements

In this project, we mainly focused on tasks 1 and 3. For task 1, we developed a scalable tree-root-like lamination at the electrode/separator interface with porous fluoropolymers, which enhances load transfer from one component to another. Such interfacial adhesion dramatically enhances the flexural modulus of pouch cells by 10 times, from 0.28 GPa to 3.1 GPa. On the other side, such modification does not compromise the electrochemical performance of corresponding cells. An NMC/graphite full cell with such interfacial lamination delivers a steady discharge capacity of 151.4 mAh g^{-1} at C/2 and 141.9 mAh g^{-1} after 500 cycles. Moreover, the specific energy only decreases by 3-4%, which is the smallest reduction reported so far in structural batteries. A prototype of "electric wings" was also demonstrated, which allows an aircraft model to fly steadily.

Besides such interfacial adhesion, we also explored multiple polymer electrolytes for enhancing load transfer when electrolyte presented, including epoxy, poly(vinyl carbonate) and polyacrylate. 10-20 X enhancement of mechanical properties are observed while electrochemical cells can be cycled. After evaluation, we decide to focus on the polyacrylate electrolyte, which will be carried in the next round of this project (2022-2024), The results are described in section 4 in the progress details.

For task 3, we performed a finite element (FE)-based model of structural batteries. The model captures mechanical properties of each component layer, interface, packaging, and external are taken into account. The model results are consistent with experiments, such as bending tests and tensile results. It also unveils the importance of external pressure on the mechanical properties of the batteries.

In addition, we also explored Task 1 and validate that Ti foils can be used as substrates to enhance mechanical properties of battery electrodes.

The major achievements include

- Developing an FE model that can appropriately describe the mechanical behavior of batteries with different mechanical properties, such as 3-point bending and tension tests.
- Developing a tree-root-like interfacial coating which laminates separators and electrodes together to enhance load transfer. The laminated cell shows a high flexural modulus of 3.1 GPa, 11 times that of a cell without interfacial lamination (0.28 GPa).
- Demonstrating an aircraft model with structural batteries as the wings and the sole power source.
- Identification of polymer electrolyte candidates with reasonable mechanical and electrochemical performance.
- Publishing five papers in high-impact journals, including one in *Advanced Energy Materials* (Impact factor IF = 29.4), one in *Joule* (IF = 41.2), one in *ACS Energy Letters* (IF = 19.1), and one in *Energy Storage Materials* (IF = 16.4), and one in *Journal of the Electrochemical Society* (IF = 4.32). One paper is under review in *Joule* (IF = 41.3).
- Writing an invited review paper on structural batteries for Materials Today (impact factor: 26.94)

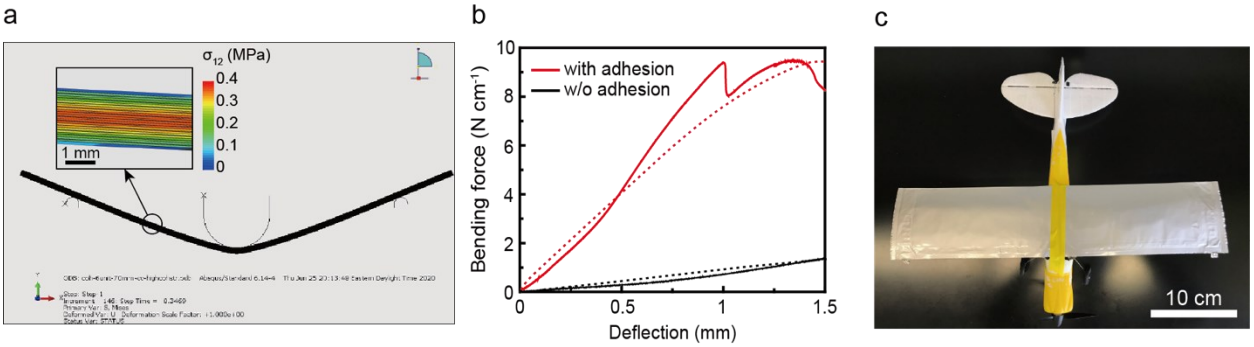

Figure 1. (a) The schematic of the FE modeling of a battery subjected to 3-point bending in Abaqus. The zoom-in image is a magnified image with stress distribution in different component layers inside. (b) Experimental bending force per width - deflection curves of 2.1 mm-thick Li-ion pouch cells with and without electrode/separator adhesion (solid lines) and corresponding FE simulation results (dotted lines). (c) The top view of an airplane model with laminated pouch cells as "electric wings". The airplane's size is 44 cm × 35 cm × 12 cm (L × W × H), and it can fly steadily with the wing cells as the only power source.

Progress Details

The progress details include four sections: 1) FE modeling of structural batteries, which describes an FEA model we built, which can serve as the digital twin to understand how batteries behave under different mechanical loads, 2) Development of tree-root-like adhesion to enhance flexural properties of batteries, 3) Prototyping of aircraft models with structural batteries-based electric wings as the power source, and 4) Polymer electrolytes for enhancing load transfer between battery components.

1. FE modeling of structural batteries.

1.1 Motivation and Model settings

Currently, the Li-ion battery is the one with the highest specific energy among different rechargeable battery systems (~250 Wh/kg).[1] Li-ion battery is a complicated system, including a stack of multiple layers of cathode, separator, and anode in sequence (Fig. 2a), which is vacuum-sealed inside a plastic pouch bag. In the cathode, cathode materials are coated onto both sides of a ~10 μm Al current collector. The cathode consists of 90-96 wt% active materials (e.g., $LiCoO_2$, $LiNi_xMn_yCo_zO_2$), 2-5 wt% carbon black, and 2-5 wt% polymeric binder. The separator is ~10-30 μm porous polyethylene with an optional 1-3 μm Al_2O_3 coating on single or both sides.[2] In the anode, the electrode layer is coated onto both sides of a ~6-8 μm Cu current collector. The electrode layer contains 92-97 wt% active materials (e.g., graphite), 2-5 wt% polymeric binder, and 1-3 wt% carbon additives. In addition, the plastic pouch is a trilayer of nylon/aluminum /polypropylene, and each layer is 20-40 μm thick.

Given the complicated structure of a commercial battery, it is very time-consuming to fabricate pouch cells for mechanical tests at the cell level, and further improve structural performance. Hence, we think that a digital twin of batteries, such as an FE model, can provide critical insights into important factors that control the mechanical properties of batteries, and examine how various strategies enhance these properties.

Based on this rationale, we developed a quasi-static 2D plane-stress finite element (FE) analysis of a Li-ion cell with multi-layer stacking inside, as shown in Fig. 1a. The model treats substrate, electrode, separator and packaging as separate layers, and their dimensions are the same as commercial cells. The electrode layer is treated as a continuous film instead of a particle-based coating. To mimic the real scenario, a typical cell in the FE model is 2.1 mm in thickness and 7 cm in length, which includes 11 layers of graphite anode and 11 layers of NMC cathode (33 mAh cm^{-2} in total).

To balance accuracy and computational cost, we ensured that each component layer has at least two 4-node quadrilateral elements (CPS4R) in its thickness direction. Frictional contact with a frictional coefficient of 0.4 is defined for electrode/separator (in models without electrode/separator adhesion) and cell/pouch interfaces.[3] All interfacial adhesion, including the electrode/current collector one and the electrode/separator one, is realized by using COH2D4 cohesive element in order to study the effect of interfacial adhesion strength on the battery's flexural properties. The boundary and loading conditions in the FE simulation are the same as the three-point bending experiments in Fig. 1a, and a mesh convergence study is also conducted. The packaging layer and the atmospheric pressure are also considered in the simulation, which is critical to mimicking the real scenario.

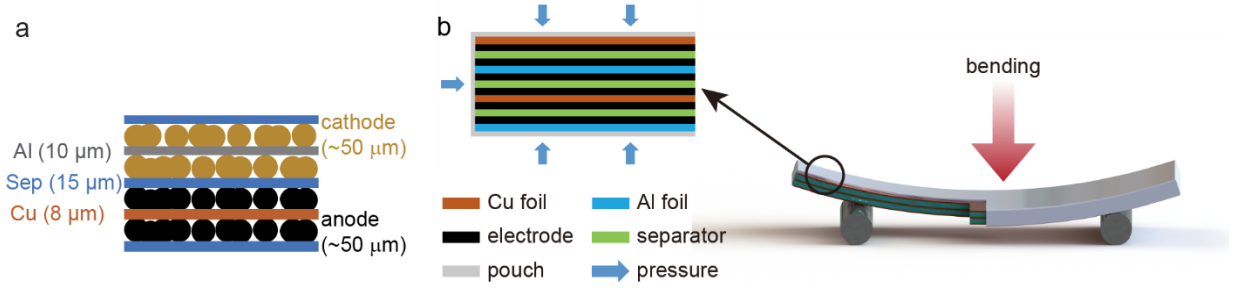

Figure 2. (a) The structure of a real Li-ion battery. (b) The cell configuration under three-point bending in finite element (FE) modeling. For clearness, only three repeating graphite/NMC units are shown, and the thicknesses of all layers are drawn to be the same. The thickness of Cu foil, graphite anode, separator, NMC cathode and Al foil are 9 μm, 60 μm, 20 μm, 60 μm and 13 μm, respectively, where active materials are coated on both sides of the metal foils.

1.3 Modeling results.

To understand how different factors affect the bending properties of a Li-ion pouch cell, we simulated the bending force-deflection curves in four cases: (A) a conventional Li-ion cell, (B) a cell with one electrode replaced by strong carbon fibers, (C) a cell with both electrodes replaced by strong carbon fibers, and (D) a conventional cell with interfacial adhesion. The results are represented in Fig. 3a.

In case A, there is no binding between electrodes and separators, and the electrode/separator interfaces are defined as frictional contact with a frictional coefficient of 0.4.[3] Due to the external atmospheric pressure, the frictional force hinders the relative sliding between electrodes and separators, but this resistance is relatively small. Therefore, at a deflection of 1 mm, the simulated bending force per width and the equivalent flexural modulus (E_f) are only 0.92 N cm^{-1} and 310 MPa, respectively.

In case B, the anode (both graphite and Cu) is replaced by stronger carbon fiber with a modulus of 230 GPa,[4] and the bending force and E_f respectively increase to 2.9 N cm^{-1} and 979 MPa at the same level of deflection. If both electrodes are replaced by carbon fiber (case C), the bending force and E_f only increase slightly to 4.1 N cm^{-1} and 1.38 GPa, respectively, which are still not satisfactory. Such poor mechanical properties arise from the relative sliding of components about frictional interfaces, and thus all components deform about their own neutral axes with poor load transfer, leading to a large compromise in flexural properties of the whole cell. The poor load transfer between different layers is also reflected by the small and discontinuous shear stress in these cells (Fig. 3c and d). These results reveal that merely improving the mechanical properties of components without addressing the interfacial sliding issue is not enough to rigidify structural batteries.

On the other hand, in case D, different battery components are bonded together as a laminate so that all components share a common neutral axis. Therefore, load transfer will be more efficient, and tremendously higher flexural modulus and stiffness can be achieved. With a moderate interfacial adhesive energy of 0.2 N cm^{-1} between an electrode and a separator, the bending force and E_f are remarkably enhanced to 8.8 N

cm^{-1} and 2.97 GPa, respectively, at a deflection of 1 mm (Fig. 3a). Fig. 3e further shows that the shear stress in such a laminated cell is much larger than that in a cell without adhesion (Fig. 3c and d), suggesting higher E_f. Moreover, the continuity of stress through all cell components also affirms good mechanical integrity and satisfying load transfer.

These results indicate that interfacial adhesion dominates the flexural modulus of a Li-ion cell, and it should be enhanced along with the mechanical properties of components themselves for realizing high-performance structural batteries.

The FEA model also shows that increasing the interfacial adhesion strength can also enhance the bending strength of a pouch cell. As shown in Fig. 3b, as the adhesion strength increases from 0.08 MPa to 0.6 MPa, the cell's flexural modulus remains the same, but the ultimate bending strength increases significantly from 9.5 N cm^{-1} to 15.6 N cm^{-1} (Fig. 3b). The deflection depth at failure also increases from 1.52 mm to 6 mm. This is because the interfacial adhesion serves to transfer the shear stress under flexing, and thus it fails when the transferred stress exceeds the adhesion strength. These results unveil that the utilization of the electrode/separator adhesion helps increase the flexural modulus of cells, while the reinforcement of the adhesion further improves the bending strength of cells.

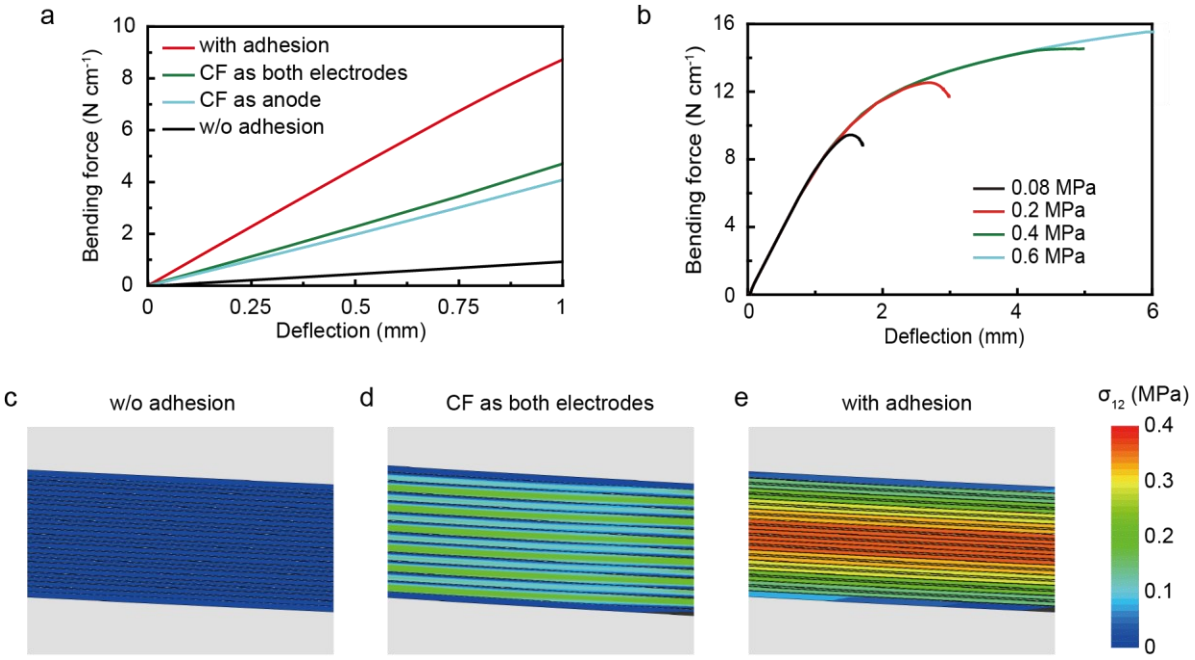

Figure 3. (a) The simulated bending force per width - deflection curves of pouch cells within a deflection of 1 mm in FE simulation. "w/o adhesion" and "with adhesion" indicate a standard Li-ion cell without and with adhesion between electrodes and separators, respectively. "CF as anode" and "CF as both electrodes" are cells with the anode and both electrodes replaced by carbon fiber (CF), respectively. (b) FE simulation of bending force per width - deflection curves of cells with different interfacial adhesion strengths. Adhesion strengths at all electrode/separator and electrode/current collector interfaces are treated to be the same for simplicity. (c-e) The simulated shear stress distributions of c) a standard Li-ion cell without adhesion between electrodes and separators, d) a cell with both anode and cathode replaced by CF, and e) a standard Li-ion cell with electrode/separator adhesion at a deflection of 1 mm. All cells are 2.1 mm thick and 7.0 cm long.

2. Development of tree-root-like adhesion to enhance flexural properties of batteries.

2.1 Fabrication processes

As suggested by the modeling above, strong adhesion between electrodes and separators is critical to enhancing the flexural properties of batteries. To achieve this goal, we developed a tree-root-like, continuous binder network at the sub-surface region of a granular electrode, which binds with a ceramic-coated separator tightly (*Advanced Energy Materials*, 2021, Fig. 4a). Such a tree-root-like structure was realized by a phase inversion method, as illustrated in Fig. 4b. First, Poly(vinylidene fluoride-co-hexafluoropropylene) (P(VdF-HFP)) was dissolved in acetone with 10 wt% water as the nonsolvent. The as-prepared solution was cast onto an NMC or graphite electrode and permeated into the porous electrode (Step 1). Upon the evaporation of acetone and water in sequence, porous P(VdF-HFP) was formed continuously among electrode particles and on the electrode surface. The thickness of the extra P(VdF-HFP) coating is 5~10 μm, which formed good adhesion to the polyvinylidene fluoride (PVdF)-Al_2O_3 composite coating on the separator during hot pressing (Step 2).

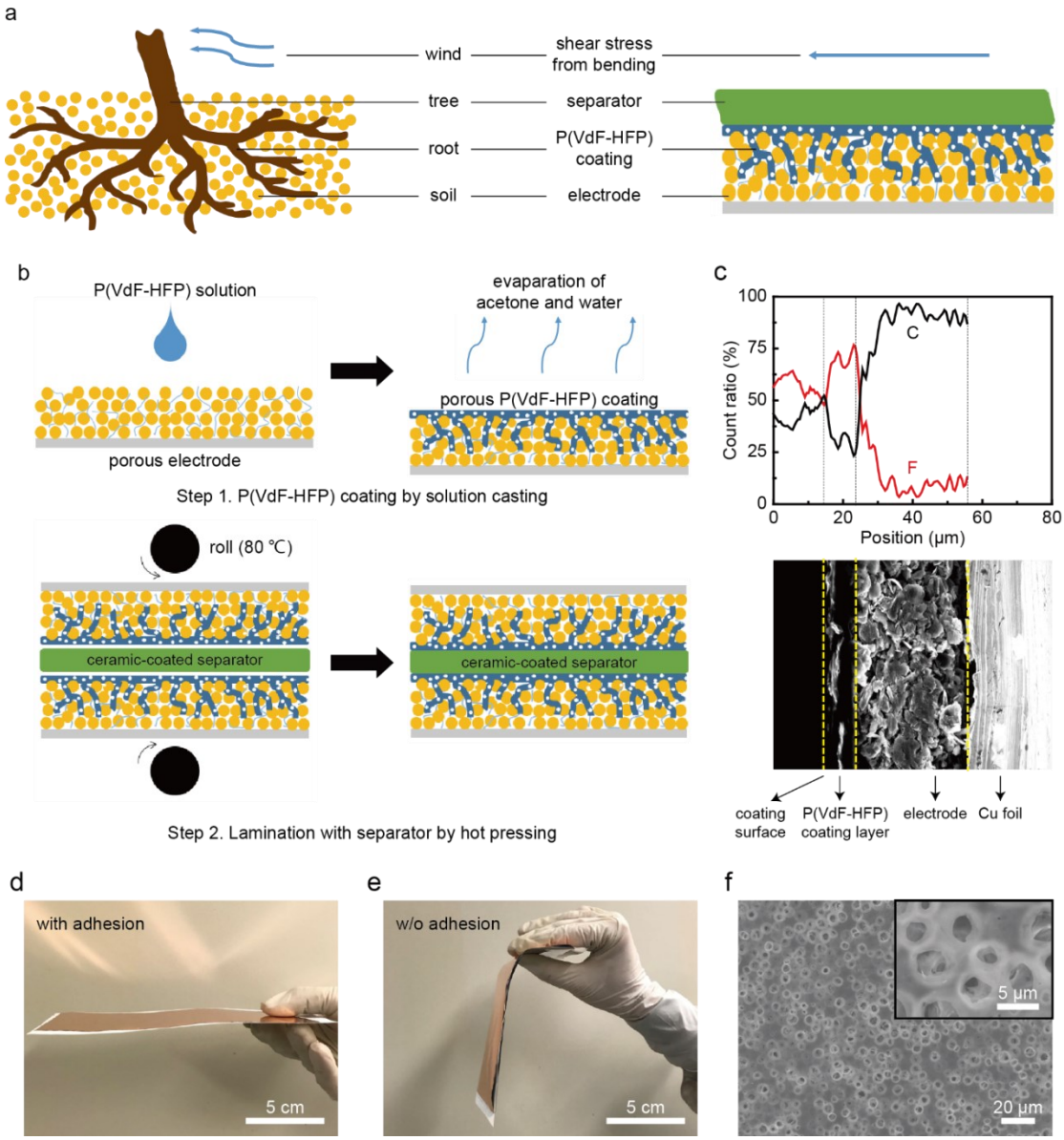

Figure 4. The design and fabrication process of a tree-root-like electrode/separator interface. (a) The analogy between a tree against strong wind (left) and the electrode/separator adhesion against shearing introduced by bending (right). (b) A schematic of the fabrication process of a structural cell with tree-root-like interfaces through hot pressing. (c) EDS line scans of C and F in a P(VdF-HFP)-coated graphite, along

with an SEM image of the region scanned. The surfaces of P(VdF-HFP) coating, electrode, and Cu current collector are marked with dash lines. (d and e) Photos of anode-separator-cathode ensembles (d) with and (e) without electrode/separator interfacial adhesion. (f) Top-view SEM images of a P(VdF-HFP) coating on an NMC electrode after adhesion.

The permeation of P(VdF-HFP) into electrodes was validated by the cross-section energy dispersive spectroscopy (EDS) line scan through an as-coated graphite electrode with sodium alginate binder (Fig. 4c). Such tree-root-like adhesion remarkably enhances the mechanical properties of batteries. As shown in Fig. 4d, a single repeating unit of an anode-separator-cathode tri-layer with such interfacial adhesion does not flex by its own weight. In contrast, without such interfacial binding, the tri-layer ensemble flexes readily by gravity due to its poor mechanical strength (Fig. 4e). In addition, the P(VdF-HFP) layer introduced is highly porous even after hot pressing, which allows ions in the electrolyte to pass readily (Fig. 4f).

2.2 Mechanical characterizations.

The P(VdF-HFP)-based interfacial adhesion significantly increases flexural properties of pouch Li-ion cells with practical sizes, and cells with dimensions of 7.0 cm × 4.0 cm × ~2.1 mm (L × W × T) and 11 graphite/separator/NMC532 repeating units inside were tested under three-point bending, whose configurations are the same as those in FE simulation (Fig. 1a) and similar with practical batteries.

First, the cell without the tree-root-like interfacial adhesion shows a low bending force of 0.72 N cm^{-1} at a deflection of 1 mm (Fig. 5a), which corresponds to an effective E_f of only 281 MPa, consistent with simulations (black dotted line in Fig. 5a) and literature reports.[5] Moreover, cell inflection near two supporting beams was observed in both simulation and experiment, which indicates relative sliding between components (Fig. 5b).

After the tree-root-like adhesion is applied, the bending force is increased by 11.5 times to 9.0 N cm^{-1} at the same deflection, and the corresponding effective E_f is as high as 3.1 GPa, which is consistent with simulations (red dotted line in Fig. 5a). This value, close to epoxy, is among the best results for structural cells with internal strengthening in the literature.[6-9] Moreover, no inflection is observed near the supporting beams in both FE simulation and experiments (Fig. 5c), further demonstrating efficient load transfer. Moreover, the processing complexity and extra packaging weights are significantly reduced compared to previously reported strategies for structural batteries.

The experimental results also align well with FE modeling, further validating our strategy that interfacial adhesion is critical to enhancing the flexural properties of Li-ion cells. The consistency between simulation and experiments also shows that modeling is a powerful approach to understand and guide experimental designs of structural batteries.

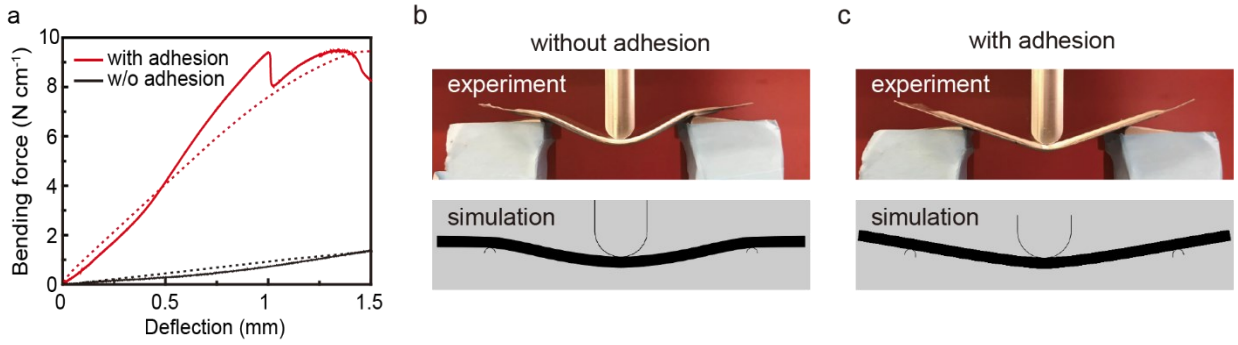

Figure 5. Mechanical properties of structural batteries with proposed interfacial lamination. (a) Experimental bending force per width - deflection curves of 2.1 mm-thick pouch cells with and without electrode/separator adhesion (solid lines) and corresponding FE simulation results (dotted lines). (b and c) The morphology of a bent cell (b) without electrode/separator adhesion and (c) with electrode/separator

adhesion in both experiment and simulation. NMC and graphite electrodes were used in these cells. The loadings in all electrodes were ~3 mAh cm^{-2}. The electrolyte amount was 2.5 g Ah^{-1}.

2.3 Electrochemical Performance

In structural batteries, the electrochemical properties should not be significantly compromised as a trade-off for enhanced mechanical properties. In our strategy, since the extra porous coating is only 5-10 mm in thickness, the mass loading of P(VdF-HFP) coating is only ~3.0 mg cm^{-2} per repeating cell unit, and thus the specific energy of a Li-ion cell is only reduced by 3% due to such a coating. This is the smallest reduction in specific energy of structural batteries in literature.[10] Moreover, P(VdF-HFP) and alginate are compatible with other components inside Li-ion cells,[11, 12] and thus, the electrochemical performance is expected to remain steady. To validate this argument, we tested both half cells and full cells with and without the tree-root-like coating layer. The areal capacities in electrochemical tests are ~1.0 mAh cm^{-2}.

Li/NMC532 and Li/graphite half-cell tests were performed first. Cells with the interfacial adhesion layer show nearly the same voltage profile and cycling performance as cells without this interfacial layer, and details can be found in our recent publication.[13]

We further tested NMC532/graphite full cells with both alginate-graphite anode and NMC532 cathode adhered to the separator (Fig. 6). After two formation cycles at C/10, the full cell was charged at C/3 and discharged at C/2. The cell showed specific discharge capacity of 148.6, 151.4, and 141.9 mAh g^{-1} in cycle 1, 100, and 500, corresponding to 95.5% capacity retention. The average CE from the 10th to 500th cycle is 99.99%. (Fig. 6a). The voltage profiles indicate that the internal resistance of the full cell with electrode /separator adhered is stable and close to the full cell without the P(VdF-HFP) adhesion (Fig. 6b and c).

Such structural full cells with interfacial adhesion layers also show reasonable rate performance. The discharge capacities are 157.7 mAh g^{-1} at C/10, 153.3 mAh g^{-1} at C/5, 149.2 mAh g^{-1} at C/3, 144 mAh g^{-1} at C/2, and 129.5 mAh g^{-1} at 1C, close to those in a cell without tree-root-like interfacial adhesion (Fig. 6d). These results demonstrate that cells with the proposed tree-root-like adhesion have reasonable electro-chemical performance and satisfactory long-term stability, and remarkably enhanced mechanical properties.

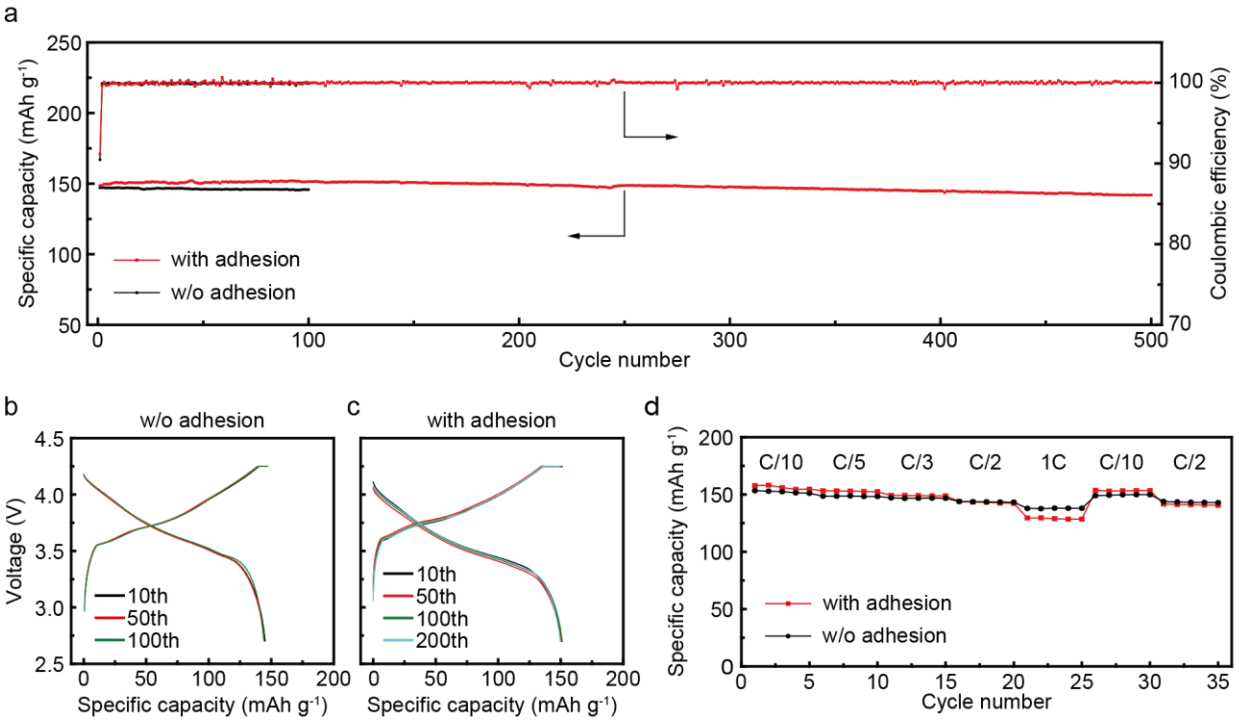

Figure 6. Electrochemical performance of structural batteries with tree-root-like interfacial adhesion and alginate binder. (a) Cycling performance of graphite/NMC532 full cells with and without electrode/separator adhesion. (b,c) Corresponding voltage profiles and (d) rate performance of graphite/NMC532 full cells. All cells were first cycled at C/10 for two formation cycles. Then they are charged at C/3 with a constant voltage step to C/20, and discharged at C/2. The mass loading is ~1 mAh cm^{-2}. The electrolyte is 1 M lithium difluoro(oxalato)borate (LiDFOB)-0.4 M lithium tetrafluoroborate ($LiBF_4$) in fluoroethylene carbonate (FEC)-diethyl carbonate (DEC) (1:2, v/v).

3. Prototype Demonstration of "Electric Wings"

To demonstrate practical applications of the proposed strategy in real devices, we replaced the wings of an aircraft model with two laminated structural pouch cells with dimensions of 23 cm × 9.0 cm × 0.6 mm (L × W × T). Each cell has a capacity of 780 mAh with two 3 mAh cm^{-2} anode-separator-cathode units, and the aircraft was solely powered by these "electric wings" (Fig. 1c and Fig. 7). With laminated cells, the aircraft model can fly steadily and smoothly, which benefits from the stiffness and lightness of the proposed structural batteries. In contrast, with conventional cells without interfacial lamination as wings, the aircraft model with the same weight falls soon after being thrown to the sky, due to the much weaker strength of the wings. Such distinctly different behaviors demonstrate the superiority of structural energy storage for light-weighting aerial vehicles.

Currently we are trying to demonstrate better designed "electric wings" which are closer to practical applications. As shown in Fig. 7c, we are currently using 3D printing to fabricate a model airplane with a wingspan of ~1.5 m, and apply structural batteries as "electric wings" for such a model airplane.

Figure 7. (a) Front view of a model airplane with laminated pouch cells as "electric wings". The airplane is 44 cm × 35 cm × 12 cm (L × W × H), and it can fly steadily with the wing cells as the only power source. A single-layer electrode is 17.3 cm × 7.5 cm (L × W) in one wing, and one wing can provide a capacity of 780 mAh. (b) The model airplane was flying in the sky, which is in the yellow circle. (c) A 3D printed airplane model with a wingspan of ~1.5 m, which serves as a platform to test structural batteries. We plan to cover the wings with structural batteries in the next step.

4. Exploration of new polymer electrolytes for enhancing load transfer

PVdF-HFP can adhere electrodes together, however, it becomes soft and less adhesive in contacting with electrolytes. Although the enhanced mechanical performance described in Fig. 5 is with electrolyte wetting, it is important to explore other polymer electrolytes to further enhance mechanical properties, especially with liquid electrolytes represented. To realize this goal, we explored multiple polymer electrolytes in year 2. After multiple failures, we identify acrylate electrolyte with a small portion of poly(vinyl carbonate) electrolyte as a potential candidate. In the following paragraphs, we will present some preliminary data on several polymer electrolyte systems we have explored, including 1) epoxy, 2) poly(vinyl carbonate), and 3) acrylate.

4.1 Epoxy electrolyte.

Epoxies are commonly used as high-performance adhesives in lightweight materials such as carbon fiber or glass fiber reinforced composites. The epoxy matrix serves as a strong binder and enables transfer of mechanical stress between laminated fiber weaves. The intrinsic mechanical properties of such epoxy adhesives can reach an elastic modulus of up to ~5 GPa and tensile strength of ~120 MPa, however, their ion conductivity is extremely low ($<10^{-6}$ S cm^{-1}), which limits their application as structural polymer electrolyte for batteries. Nevertheless, there have been many approaches to blend epoxies with ionic liquids or liquid electrolytes for improving their ion conductivity and at the same time sacrificing some mechanical performance.

In our investigation, we used bisphenol-A diglycidyl ether (BADGE) as resin component and triethylenetetramine (TETA) as hardener component for the epoxy system. We were able to obtain a porous membrane (Fig. 8a), where the mechanical properties were dependent on the amount of network expander poly(ethylene glycol) diglycidyl ether (PEGDGE) and pore forming agent poly(ethylene glycol) (PEG) and significantly decreased compared to the reference as it is shown in Fig. 8b. The porosity was obtained by dissolving the PEG after the polymerization of the membrane.

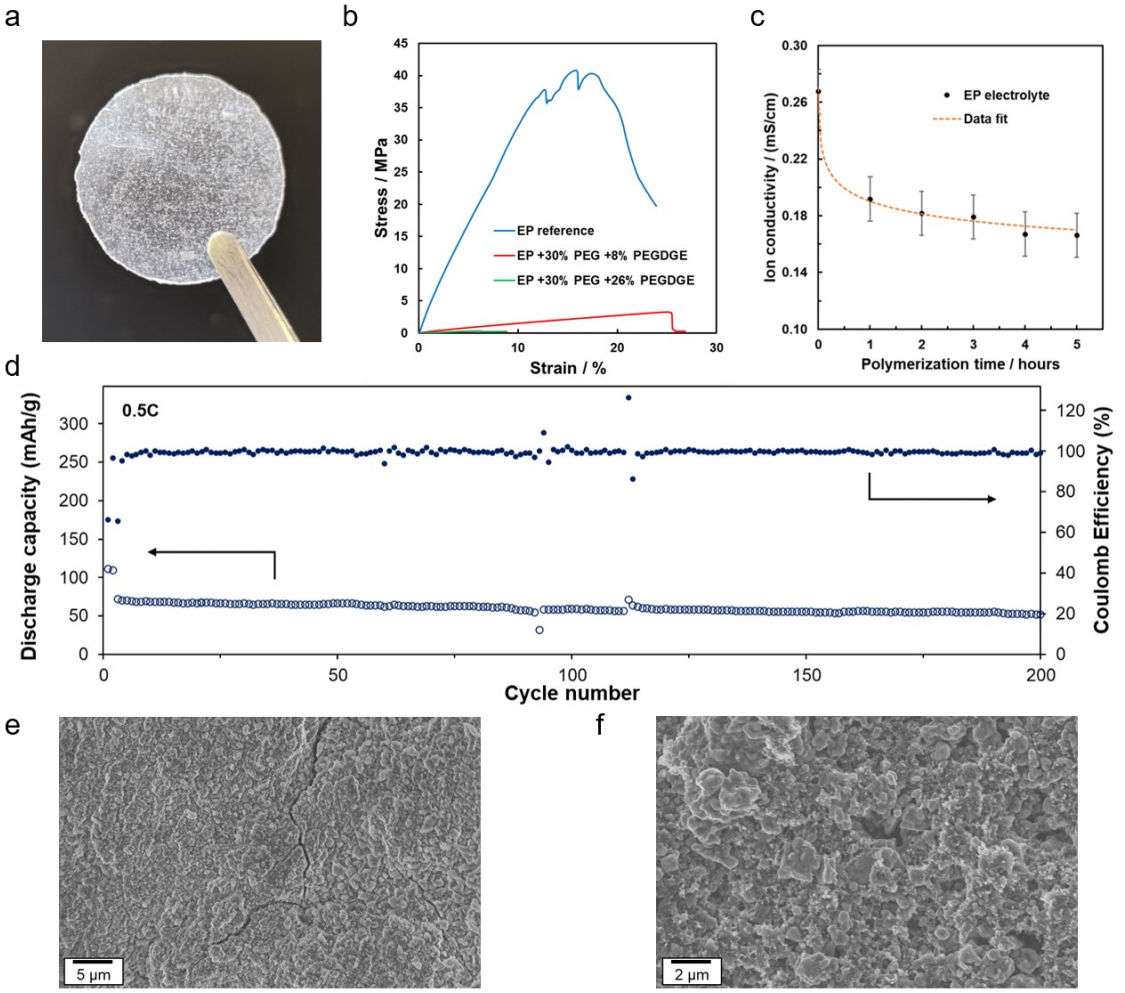

Figure 8. (a) Porous epoxy-based membrane. (b) Tensile tests of an epoxy reference and epoxy-based electrolytes. (c) The ion conductivity of an epoxy electrolyte depending on the polymerization time. (d) Cycling data of a Li/$LiFePO_4$ (LFP) cell with epoxy-based electrolyte at room temperature with 0.5 C discharge rate. (e-f) SEM images of an LFP electrode covered with epoxy electrolyte after *in-situ* polymerization.

The epoxy-based electrolytes could reach sufficiently high ion conductivity (~10^{-4} S cm^{-1}) by soaking porous epoxy-based membranes in liquid electrolyte such as 1M $LiPF_6$ in 1:1 EC/DEC (Fig. 8c). Such an external polymerization is referred to as *ex-situ* approach. For an effective load transfer between cell components, an internal polymerization would be much more beneficial since the cell components would be integrated into the polymer (*in-situ* approach). Several attempts of in-situ polymerizations have been carried out, but no sufficiently high specific capacity could be achieved so far (Fig. 8d). SEM images revealed good interconnection of the epoxy with the electrode surface and coverage of cathode particles (Fig. 8e-f), which is believed to cause increased resistance during the cycling tests. Given the low specific capacity, we decide not to pursue this system.

4.2 Poly(vinyl ethylene carbonate)

Vinylethylene carbonate (VEC) is a frequently used additive for liquid electrolytes to improve the solid electrolyte interface (SEI) layer stability. It can be polymerized to form poly(vinyl ethylene carbonate) (PVEC) using thermal radical initiators like azobisisobutyronitrile (AIBN). PVEC was reported as polymer electrolyte with high ion conductivity of up to 1.35 mS cm^{-1} and good compatibility with Li anode and LFP or LCO cathodes [14]. Compared to other polycarbonates the higher ion conductivity of PVEC is due to the flexibility of the ethylene carbonate (EC) side groups of the polymer chain, which can rotate freely as it is shown in Fig. 9a.

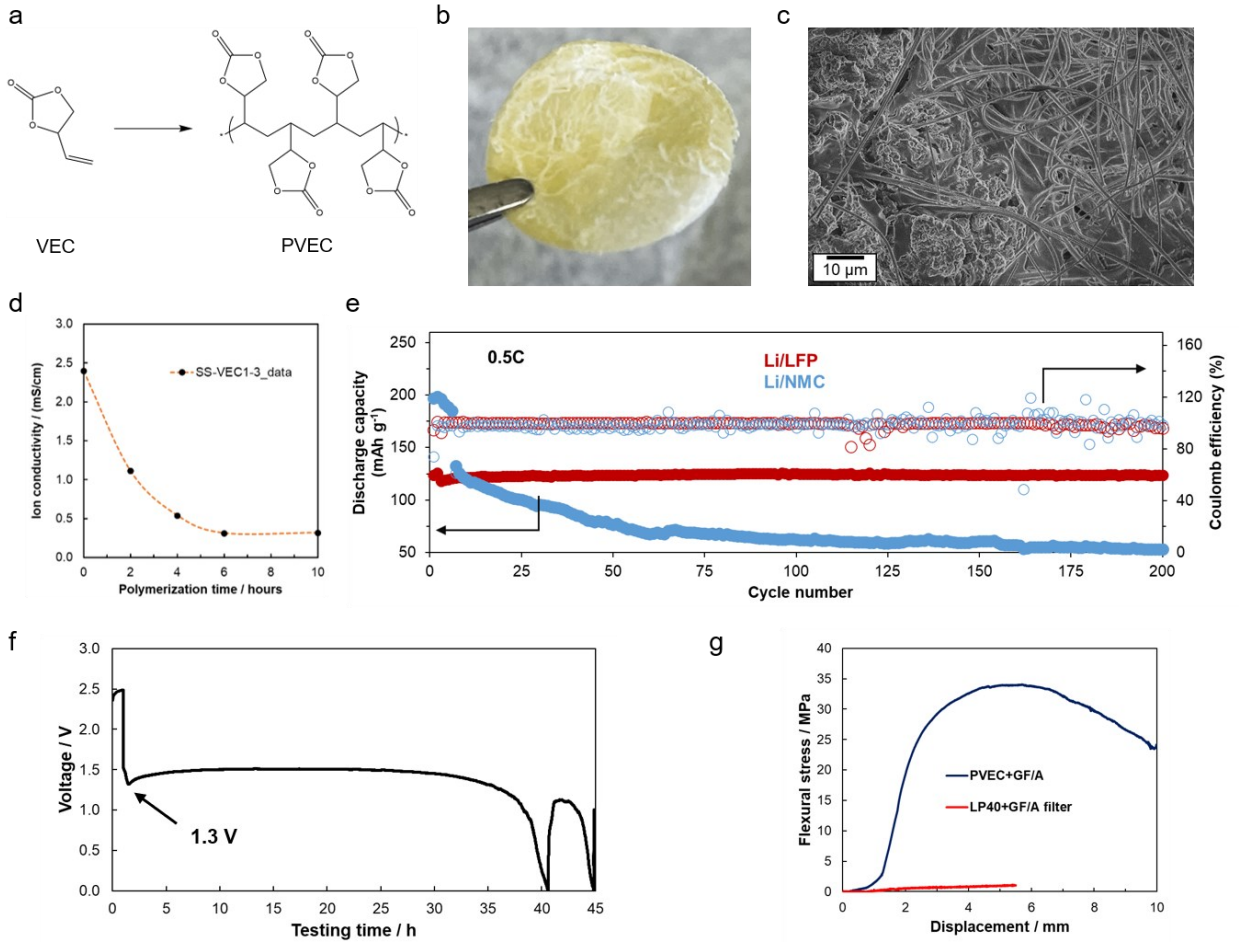

Figure 9. (a) Chemical formulas of the polymerization reaction of VEC to PVEC. (b-c) Photo and SEM image of PVEC on GF separator after the polymerization. (d) The ion conductivity of the PVEC electrolyte in a stainless-steel symmetric cell depending on the polymerization time. (e) Long-term cycling tests with PVEC electrolyte of a Li/LFP and a Li/NMC cell at room temperature. (f) Voltage profile of a Li/graphite

cell with indicated post-polymerization of VEC starting at about 1.3 V during the first cycle. (g) Three-point pending test of 1 unit cell with PVEC and GF separator compared to liquid electrolyte (LP40, 1 M $LiPF_6$ in ethylene carbonate and diethyl carbonate 1:1).

In our experiments, VEC monomer was mixed with 30 %wt LiTFSI salt, 1 %wt AIBN and combined with a glass microfiber (GF) separator (Fig. 9b-c). The polymerization was performed *in-situ* inside coin cells with Li anode and LFP/NMC cathode at 80°C until a solid polymer electrolyte was obtained after >8 h, resulting in an ion conductivity of ~0.3 mS cm^{-1} (Fig. 9d). The Li/LFP cells delivered reasonably high specific capacity of ~125 mAh g^{-1} and good cycling stability over 200 cycles, however, with Li/NMC the capacity of the cell degraded quickly (Fig. 9e) and post-polymerization was observed with Li/graphite (Fig. 9f), which could be explained by incomplete polymerization. Further attempts of longer polymerization time and higher temperatures could not solve this issue.

The mechanical performance of 1 unit cell, consisting of anode (graphite/Cu), PVEC electrolyte with GF separator and cathode (LFP/Al) was measured via three-point bending tests. It could be shown that by replacing a liquid electrolyte (LP40, 1 M $LiPF_6$ in ethylene carbonate and diethyl carbonate 1:1) by the solid PVEC electrolyte the elastic modulus and flexural strength could be improved from 184 MPa and 1.2 MPa to 7700 MPa and 34.1 MPa, respectively (Fig. 9g).

In summary, the PVEC electrolyte demonstrates high potential for the mechanical reinforcement of batteries but could only successfully applied in Li/LFP cells. The low stability against reduction at low potential with graphite and oxidation with the high voltage cathode NMC substantially limits its practical application for structural batteries. Therefore, further experiments are focused on different polymer electrolyte systems.

4.3 Acrylate-based electrolyte

Polyacrylates are thermoplastics with a wide variety of physical and chemical properties depending on the monomers and polymerization conditions. For specific requirements different monomers can be co-polymerized to tailor the properties. Acrylates are typically used in paint, adhesive, acrylic elastomers or acrylic glass. Different arylate-based electrolyte systems have been studied for application in batteries in combination with Li-salts. The monomers can be mono- or multifunctional depending on the number of unsaturated groups and form polymer chains in case of 1-2 double bonds or 3D crosslinked networks if 3 or more double bonds are available in the monomer. Their appearance is strongly connected to the crosslinking degree and ranges from soft gels to rigid solids.

In our study, different amounts of trimethylolpropane triacrylate (TMPTMA) were blended with 1 %wt AIBN and a liquid electrolyte mix (1M $LiPF_6$ in 1:1 vol EC/DEC) to achieve a solid polymer electrolyte with high ion conductivity. Due to the presence of 3 double bonds in the monomer, the polymerization can be carried out at relatively low temperatures (<60°C). A mix of 10 %wt TMPTMA and liquid electrolyte can be fully polymerized at 55°C within ~8 h (Fig. 10a). Three-point bending tests of such an electrolyte indicate an elastic modulus of 180 MPa and a flexural strength of 2.7 MPa (Fig. 10b). Combined with electrodes and a GF separator, the mechanical performance of 1 unit cell can be significantly improved from a modulus of 168 MPa to 12.5 GPa, as it is shown in Fig. 10c, which indicate an efficient stress transfer between the electrodes.

Initial electrochemical impedance tests show that the ion conductivity of the arcylate-based electrolyte can reach ~0.7 mS cm^{-1} at room temperature after the *in-situ* polymerization in a Li/LFP coin cell with a GF separator (Fig. 10d). The acrylate electrolyte demonstrates good cycling stability with Li/LFP and Li/NMC (Fig. 10e). Currently, different electrolyte formulations are under investigation to improve the capacity retention with a NMC cathode and the compatibility with the graphite anode.

Overall, the acrylate-based electrolyte shows promising results in both aspects, mechanical and electrochemical performance. The application of this polymer electrolyte in structural batteries will be further investigated.

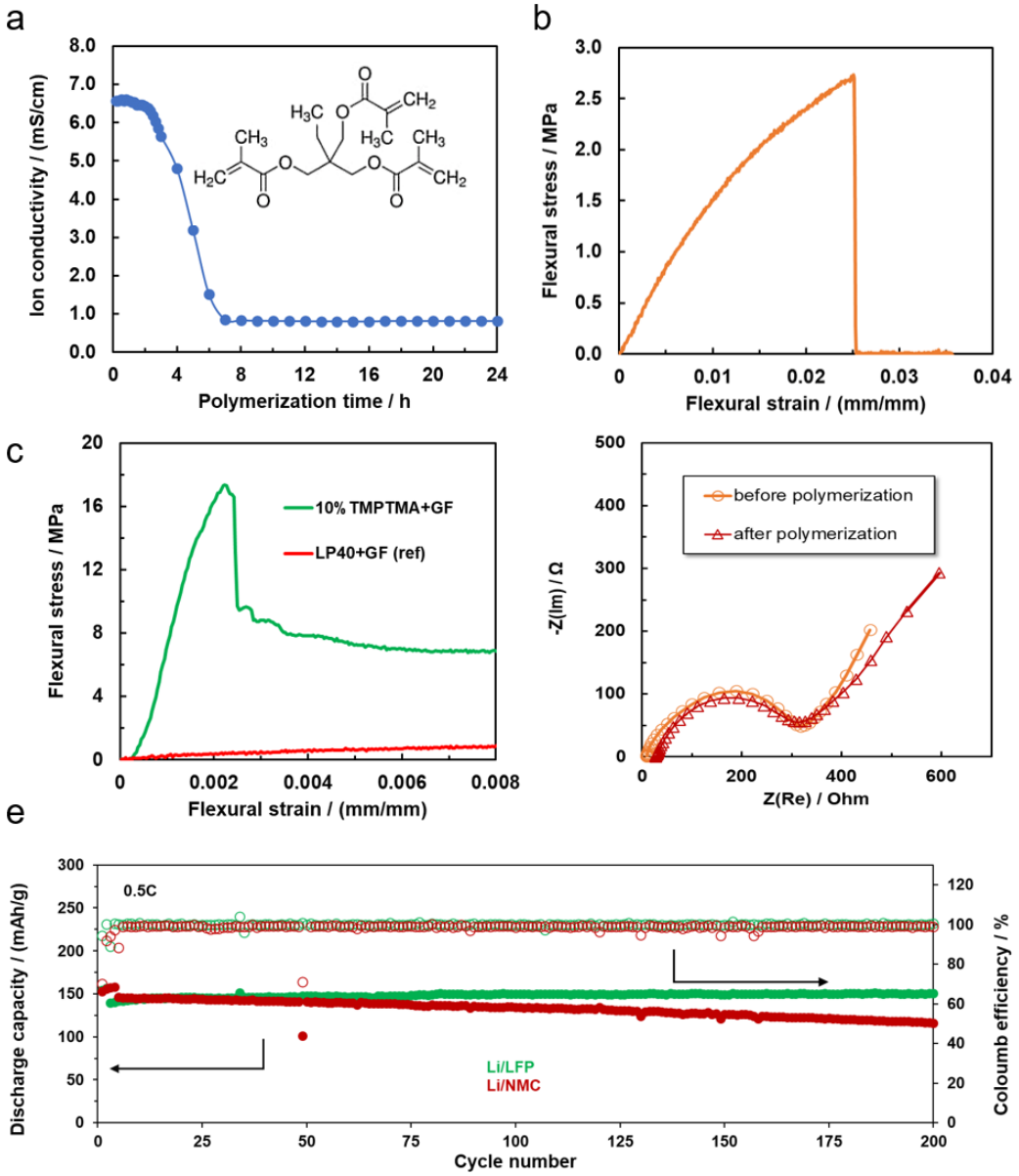

Figure 10. (a) The ion conductivity of the acylate electrolyte based on 10 %wt TMPTMA monomer depending on the polymerization time at 55ºC. (b) Three-point pending test of pure acrylate electrolyte and (c) after combining in 1 unit cell with GF separator compared to liquid electrolyte (LP40). (d) Nyquist plot of a Li/LFP coin cell with acrylate electrolyte and GF separator before and after the *in-situ* polymerization. (e) Long-term cycling tests of Li/LFP and Li/NMC cells with acrylate electrolyte at room temperature.

Publication list

AFOSR grant has a major contribution:

1. T. Jin, Y. Ma, Z. Xiong, X. Fan, Y. Luo, Z. Hui, X. Chen, **Y. Yang***, Bio-inspired, Tree-Root-like Interfacial Designs for Structural Batteries with Enhanced Mechanical Properties. *Advanced Energy Materials*, 11, 2100997 (2021)
2. W. Huang, P. Wang, X. Liao, Y. Chen, J. Borovilas, T. Jin, A. Li, Q. Cheng, Y. Zhang, H. Zhai, A. Chitu, Z. Shan, **Y. Yang***, Mechanically-robust structural lithium-sulfur battery with high energy density. Energy Storage Materials, 33, 416-422 (2020). (This one was incorporated in the report for grant FA9550-18-1-0410 since the data were obtained by the end of this project).
3. T. Jin, G. Singer, K. Liang, **Y. Yang***, Structural Batteries: Advances, Challenges and Perspectives, Materials Today, in preparation (invited review)

AFOSR grant has a minor contribution:

4. R. Choudhury, J. Wild, **Y. Yang***, Engineering Current Collectors for Batteries with High Specific Energy. *Joule*, 5, 1301-1305 (2021).
5. Z. Li, H. Zhang, X. Sun, **Y. Yang***, Mitigating Interfacial Instability in Polymer Electrolyte-based Solid-State Lithium Metal Batteries with 4V Cathodes. *ACS Energy Letters*, 3244-3253 (2020).
6. T. Xu, C. Chen, T. Jin, S. Lou, R. Zhang, X. Xiao, X. Huang, and **Y. Yang***, Chemical Heterogeneity in PAN/LLZTO Composite Electrolytes by Synchrotron Imaging, Journal of The Electrochemical Society, 168, 110522 (2021)
7. J.C. Russell, V.A. Posey, J. Gray, R. May, D. A. Reed, H. Zhang, L. E. Marbella, M.L. Steigarwald, Y. Yang, X. Roy, C. Nuckolls, and S. R. Peurifoy, High-performance organic pseudocapacitors via molecular contortion, *Nature Materials*, 20, 1136 (2021).
8. Q. Cheng*, T. Jin, Y. Miao, Z. Liu, J. Borovilas, H. Zhang, S. Liu, S. Kim, R. Zhang, H. Wang, X. Chen, L. Chen, J. Li, W. Min* and **Y. Yang***, Stabilizing lithium plating in polymer electrolytes by concentration-polarizationinduced phase transformation, *Joule*, in revision.

References

1. Misra, A. Summary of 2017 NASA Workshop on Assessment of Advanced Battery Technologies for Aerospace Applications. (2018).
2. Jung, Y.S. et al. Improved functionality of lithium-ion batteries enabled by atomic layer deposition on the porous microstructure of polymer separators and coating electrodes. *Advanced Energy Materials* **2**, 1022-1027 (2012).
3. Li, W., Zhu, J., Xia, Y., Gorji, M.B. & Wierzbicki, T. Data-Driven Safety Envelope of Lithium-Ion Batteries for Electric Vehicles. *Joule* **3**, 2703-2715 (2019).
4. Kjell, M.H., Jacques, E., Zenkert, D., Behm, M. & Lindbergh, G. PAN-Based Carbon Fiber Negative Electrodes for Structural Lithium-Ion Batteries. *Journal of the Electrochemical Society* **158**, A1455-A1460 (2011).
5. Ladpli, P., Nardari, R., Kopsaftopoulos, F. & Chang, F.K. Multifunctional energy storage composite structures with embedded lithium-ion batteries. *Journal of Power Sources* **414**, 517-529 (2019).
6. Liu, P., Sherman, E. & Jacobsen, A. Design and fabrication of multifunctional structural batteries. *Journal of Power Sources* **189**, 646-650 (2009).
7. Thakur, A. & Dong, X. Printing with 3D continuous carbon fiber multifunctional composites via UV-assisted coextrusion deposition. *Manufacturing Letters* **24**, 1-5 (2020).
8. Moyer, K. et al. Carbon fiber reinforced structural lithium-ion battery composite: Multifunctional power integration for CubeSats. *Energy Storage Materials* **24**, 676-681 (2020).
9. Thomas, J.P. & Qidwai, M.A. Mechanical design and performance of composite multifunctional materials. *Acta Materialia* **52**, 2155-2164 (2004).
10. Hopkins, B.J., Long, J.W., Rolison, D.R. & Parker, J.F. High-Performance Structural Batteries. *Joule* **4**, 2240-2243 (2020).
11. Kovalenko, I. et al. A Major Constituent of Brown Algae for Use in High-Capacity Li-Ion Batteries.

Science **334**, 75 (2011).
12. Jin, T. et al. Nonflammable, Low-Cost, and Fluorine-Free Solvent for Liquid Electrolyte of Rechargeable Lithium Metal Batteries. *ACS Appl Mater Interfaces* **11**, 17333-17340 (2019).
13. Jin, T. et al. Bioinspired, Tree-Root-Like Interfacial Designs for Structural Batteries with Enhanced Mechanical Properties. *Advanced Energy Materials* **n/a**, 2100997.
14. Wang, Y. et al. Hydrogen bonds enhanced composite polymer electrolyte for high-voltage cathode of solid-state lithium battery. *Nano Energy* **96**, 107105 (2022).